PETROPHYSICS, VOL. 54, NO. 2 (APRIL 2013); PAGE 76–90; 26 FIGURES; 2 TABLES

New Approach to Interpretation of NMR Logs in a Lower Cretaceous Chalk Reservoir[1]

Wim Looyestijn[2] and Stefan Steiner[3]

ABSTRACT

NMR logs taken over hydrocarbon intervals show significant differences with routine core data. Ideally, one should do laboratory NMR at full reservoir conditions, which is very expensive. As an alternative, we propose that the same can be modeled, starting from routine NMR on core, and estimated values of oil properties and saturation. The advantage of this approach is that changes in these estimates can easily be made. The modeled NMR response is then used to calibrate interpretations such as bound water, permeability and capillarity.

Another new concept is a variable, rather than a fixed, $T_{2cutoff}$ for the prediction of bound water from the NMR log. In-situ modeling was also used to calibrate this cutoff against features of the actual log.

We show that the actual log response is faithfully predicted by our modeling for two wells in the Valdemar area. Well A was drilled with water-based mud (WBM) and logged with a wireline NMR tool, and Well B was drilled with oil-based mud (OBM) and logged with an LWD NMR tool.

The results compare generally well with the resistivity-derived saturation, but local deviations are found. Similarly, permeability correlations calibrated to in-situ conditions produced values that compare favorably with core data where available. Pseudo-capillary-pressure curves computed from the NMR log, using calibration against available core data, were used to locate the free-water level (FWL). Wettability was assessed from the shift of the oil-relaxation time away from its predicted bulk value under reservoir conditions. The reservoir appears to be strongly water-wet.

INTRODUCTION

It is well known that interpretation of NMR logs on the basis of core-derived parameters often fails because the downhole situation is much different from that in the laboratory. The largest difference is usually caused by the presence of hydrocarbons (at some remaining saturation). In addition to this, logging tools always measure in an inhomogeneous magnetic field, which may introduce diffusion effects. Core measurements at full in-situ conditions are possible, in principle, but very expensive and therefore bound to span a limited range of properties.

We demonstrate that the same can be achieved by forward modeling of the NMR response. The starting point is a representative set of water-saturated core samples measured at ambient conditions. Forward modeling then introduces changes in the NMR response corresponding to full in-situ conditions, including effects due to the presence of native hydrocarbons, mud-filtrate invasion and wettability. Specific hardware features of logging tools, such as their gradient and acquisition parameters, are also included. Interpretation parameters, such as (variable) $T_{2cutoff}$, and permeability exponents can now be calibrated on NMR data as they appear on the log. Once the workflow has been set up, any change in conditions is automatically translated in an update of the interpretation parameters; this would not be possible with laboratory experiments.

We apply this approach to NMR logs taken in a chalk field in the Danish section of the North Sea. The Lower Cretaceous Sola and Tuxen formations lie conformably on the mainly tight Valhall formation. The heterogeneous reservoir is composed of argillaceous chalks and marly chalks with thin marlstone and shale beds, sealed by Albian shale and the tight lower part of the Upper Cretaceous chalks above. The argillaceous chalk, marl and claystone of the Sola and Tuxen Formations, which now host the hydrocarbons, were deposited over a period of 10 million

Manuscript received by the Editor November 26, 2012; revised manuscript February 28, 2013.
[1] Originally presented at the SPWLA 53rd Annual Logging Symposium, Cartagena, Colombia, June 16-20, 2012, Paper HH
[2] Formerly with Shell International, The Netherlands, currently private consultant; Email: wim@wimlooyestijn.com
[3] Formerly with Maersk Olie og Gas, A.S., currently with ADCO; Email: ssteiner@adco.ae

years during Hauterivian, Barremian and Aptian time (all Early Cretaceous). The study area is situated in the central part of the Danish Central Graben in the North Sea at a junction between the Tail End Graben (North) the Salt Dome Province (South) and the Arne-Elin Graben (Northwest). The field is situated on the crest of an inversion anticlinal ridge along a north-south trending fault system with an assumed four-way dip closure. The Lower Cretaceous oil accumulation is continuous across this whole area. To the north, the anticlinal ridge structure drops slowly, but oil saturations drop very quickly. To the south, the structure drops slowly and then rises again to form another structure less than 5 km to the south.

IN-SITU MODELING OF NMR RESPONSE

Largely for the purpose of wettability determination from NMR, very detailed modeling capability to simulate the NMR response under actual in-situ conditions, including wettability (Looyestijn et al., 2005) and acquisition settings (Slijkerman et al., 1999) has been developed in the recent past.

The effect of (remaining) oil saturation, field gradient and wettability on the NMR response is illustrated for Sample 1. Figure 1 shows the measured response at S_w = 1 as a single peak (blue curve). The simulated response at partial oil saturation (S_w = 0.7) is shown as the red curve. The oil response appears as a peak at around 4 sec, which is the value for the live crude at reservoir conditions in this field (Lo et al., 2000). Notice that the water response, below 10 msec, has not only reduced amplitude (because S_w = 0.7), but is also shifted to lower T_2 values. This is caused by the partial desaturation of the pores: the water volume is now reduced, while the surface area has remained the same; the pore responds as if it were smaller, and thus has a shorter T_2.

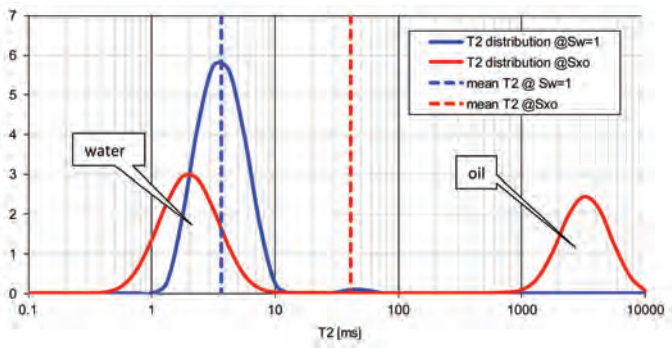

Fig. 1—Forward modeling of NMR response of Sample 1 at S_w = 0.7, no gradient, water-wet.

The next step is modeling the effect of a magnetic field gradient (Fig. 2).

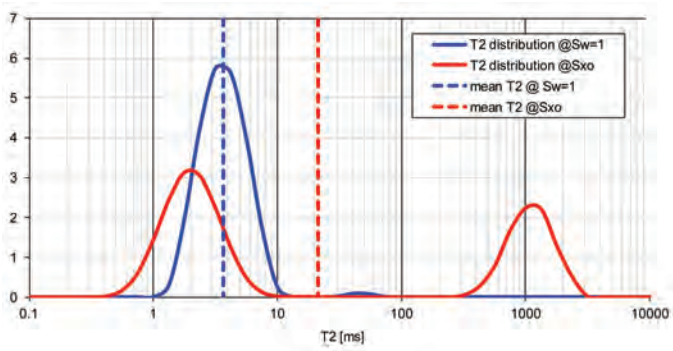

Fig. 2— Forward modeling of NMR response of Sample 1 at S_w = 0.7, gradient of 22 G/cm, water-wet.

This so-called diffusion effect is seen as an apparent relaxation rate, and adds up to the normal relaxation in a reciprocal fashion:

$$\frac{1}{T_{2,apparent}} = \frac{1}{T_2} + \frac{1}{T_{2,D}} \quad (1)$$

This formula shows that for a given magnitude of the diffusion effect, $T_{2,D}$, it will have a significant impact if T_2 is long, but hardly noticeable when T_2 is small. Hence, turning on a field gradient is predominantly seen at the right side of the T_2 distribution. It is assumed that the rock has no internal field gradient. Diffusive coupling is ignored.

Thus far the modeling assumed that the rock is fully water-wet. However, if this condition is not true, the oil will have contact with a fraction of the rock surface, and thus gets an accelerated relaxation. As a rule of thumb, a fully oil-wet condition would cause the oil to be shifted to approximately the position of the water peak (in reality roughly a factor 3 higher because the oil has a lesser surface relaxivity). The large distance of some two decades between the responses at these two extreme conditions makes the wettability determination very easy in this field.

The NMR wettability index, *NWI*, is defined in analogy with the Amott scale as +1 for water-wet, 0 for neutral/intermediate, to -1 for oil-wet (Looyestijn et al., 2005). As explained in this reference, only the ratio of the surface relaxivity to oil and to water is required; this ratio was taken as 0.3.

Figure 3 shows that even a very small deviation from water-wet causes a noticeable shift of the oil peak (in fact, to a position as seen on the NMR log in well A). To shift the peak to a much lower value still requires no more than *NWI* = 0.90 (Fig. 4). Finally, at a neutral-to-intermediate wettability (*NWI* = 0), the oil peak has merged into the water peak and cannot be discerned as a separate peak (Fig. 5).

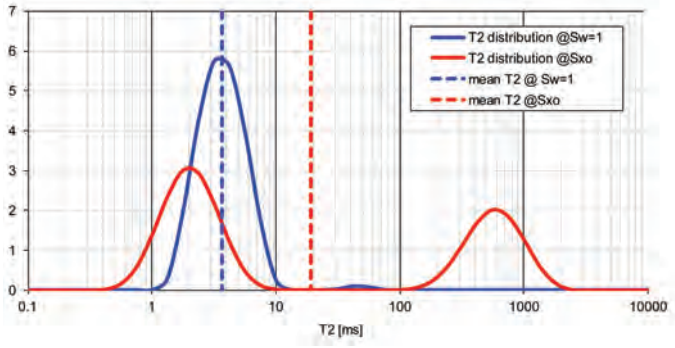

Fig. 3—Forward modeling of NMR response of Sample 1 at S_w = 0.7, gradient of 22 G/cm, at wettability index of 0.99 (very strongly water-wet).

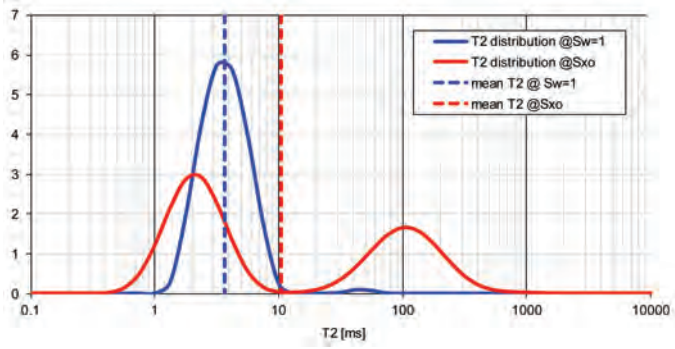

Fig. 4—Forward modeling of NMR response of Sample 1 at S_w = 0.7, gradient of 22 G/cm, at wettability index of 0.90 (strongly water-wet).

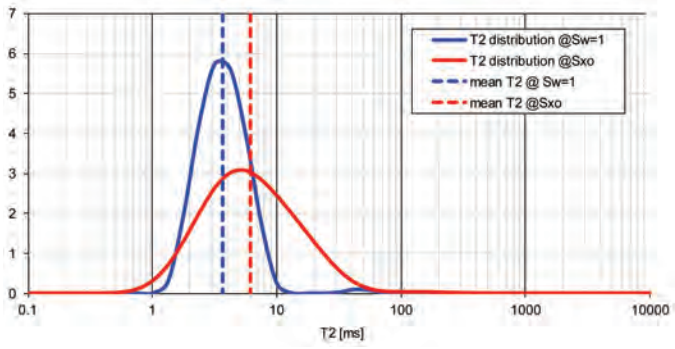

Fig. 5—Forward modeling of NMR response of Sample 1 at S_w = 0.7, gradient of 22 G/cm, at wettability index of 0.0 (neutral wet).

The use of oil-based mud, OBM, in well B has a different effect on the NMR log than water-based mud, as used in well A. In the latter case, water filtrate displaces some of the crude and partly restores the water peak to the S_w = 1 situation.

OBM filtrate, on the other hand, is an oil phase with a T_2 typically at a few hundred msec. The water peak will not change as long as the oil filtrate displaces part of the crude oil. Depending on the amount of filtrate, all of the crude may be displaced, or only some; in the latter case it may mix with the filtrate. The NMR response of a mix has a T_2 approximately given by the logarithmic mean of the two components, weighted by the relative fraction. Most OBM types consist primarily of a mix of alkenes in the C_{15} to C_{18} range. These oils have a hydrogen index of approximately unity under normal reservoir conditions; this means that the NMR porosity is not affected by OBM.

A further complication is that OBM contains emulsifiers to keep the water in the oil. These emulsifiers render the rock that is exposed to them oil-wet. In principle, a mudcake prevents emulsifiers to invade the rock, but in order to build a mudcake, some unfiltered fluid has to invade. Depending how fast a mudcake is formed, wettability alteration towards more oil-wet may occur at the depth into the formation where the NMR log reads (typically a few inches).

Figure 6 shows the predicted response for the case that no wettability alteration is seen. Since the oil filtrate and the crude peaks are close to each other, they may not be seen as separate peaks, but rather merge into a single broad hump. The good news is that the water peak is clearly separated from the oil. As long as the filtrate does not enter the rock at high overpressure, the water saturation remains unchanged, and the NMR log gives a simple means to determine the water volume, and thus saturation.

The response will be much different if significant wettability alteration occurs. Figure 7 shows the situation where the wettability has changed to intermediate (neutral). In such a situation water and oil cannot be discriminated on the basis of T_2 alone and more advanced measurements (diffusion) are required (Slijkerman et al., 1999).

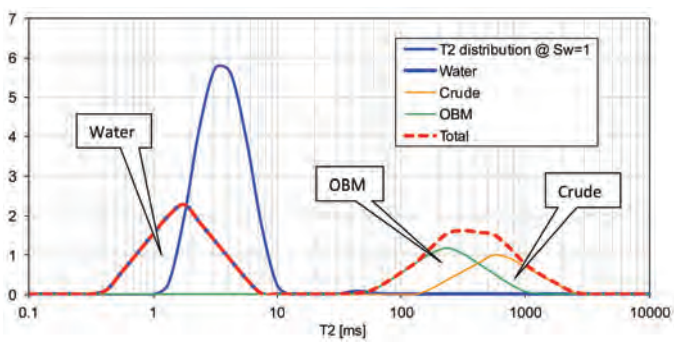

Fig. 6—Simulated response for OBM condition without wettability alteration.

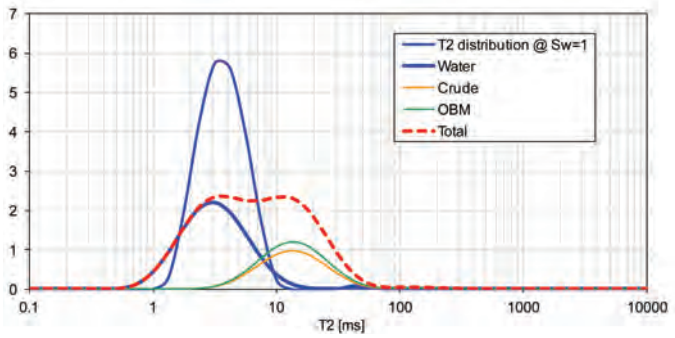

Fig. 7—Simulated response for OBM condition with wettability altered to intermediate.

VARIABLE $T_{2cutoff}$ FOR BOUND WATER

Statement of the Problem. While the concept of a fixed $T_{2cutoff}$ has been very successful for sandstones, it often fails in carbonates. This is illustrated in Fig. 8, which shows the T_2 distribution of a carbonate sample (not from this study), measured at full water saturation, and after desaturation in a centrifuge to irreducible saturation. The $T_{2cutoff}$, by definition, is the T_2 value for which the area under the S_w = 1 curve equals the entire area under the S_{wirr} curve. This sample has a $T_{2cutoff}$ of 350 msec. Fig. 9 shows another sample from the same field, with a $T_{2cutoff}$ of only 14 msec. It is clear that any single cutoff value produces gross errors in the prediction of bound water: because the distributions are rather narrow, a small change in $T_{2cutoff}$ has a dramatic effect on the predicted value of bound water.

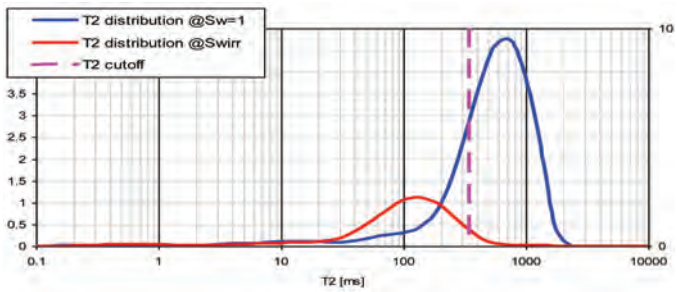

Fig. 8—Example of a high-permeability rock with a high $T_{2cutoff}$.

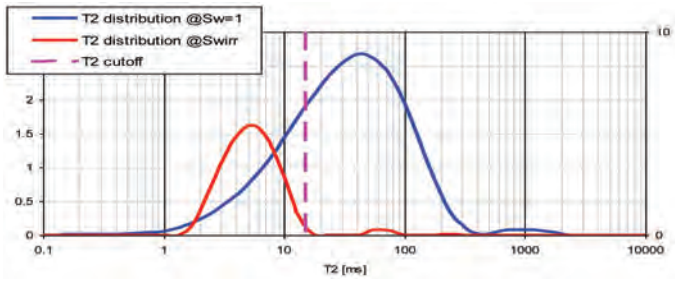

Fig. 9—Example of a low-permeability rock with a low $T_{2cutoff}$.

Proposed Solution: Variable Cutoff. If a single, average, $T_{2cutoff}$ does not work, the obvious solution would be to use a variable cutoff. This cutoff can readily be determined on core samples when the bound-water saturation is known. The challenge, however, is to find a way to predict the correct value of the cutoff without having to measure the bound-water volume. Analysis of our large in-house carbonate NMR database suggests the existence of a fairly good correlation between the $T_{2cutoff}$ and the logarithmic mean of the water peak in the distribution, T_{2peak}. This correlation exists for the present dataset, as is shown in Fig. 10. However, this is only valid for fully water-bearing rock (S_w = 1).

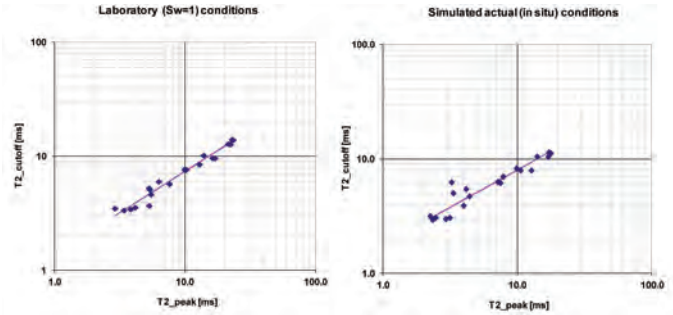

Fig. 10—Correlation of $T_{2cutoff}$ and T_{2mean} under laboratory (left) and in-situ (right) conditions.

Note that this variable cutoff is a distinctly different concept than a "tapered cutoff" or "spectral BVI" as used by logging service companies. These concepts employ a gradual split, or soft cutoff, between bound and free fluid, rather than a hard cutoff; however, this cutoff is still fixed at one particular T_2. The variable cutoff, on the other hand, does change between samples on the basis of a suitable parameter. Moreover, it can be applied either as a soft or a hard cutoff.

The name "variable cutoff" is sometimes used to fit the resistivity-derived saturation. However, that approach undermines the value of NMR as an independent verification of bound water. The concept shown here does have a predictive power because it remains independent of the (deep) resistivity.

Complication if $S_w \neq 1$. As it happens, most NMR logs are taken in situations where the rock is not fully water saturated, but contains a certain amount of hydrocarbons. The effect of this on the NMR signal is complicated, but fairly well understood.

We applied our modeling now to simulate the NMR response of the core samples as it would be seen by the NMR log under the conditions prevailing in this well. The modeling result is shown in Fig. 11; to the left the situation at S_w = 1, and to the right at reservoir condition. The S_{xo} and wettability values were taken from the NMR log interpretation presented later in this paper. As discussed above, it can be observed that

the water peak of all samples has shifted slightly to shorter T_2, and has reduced amplitude; both effects are due to the partial replacement water by (residual) oil, which appears at long T_2.

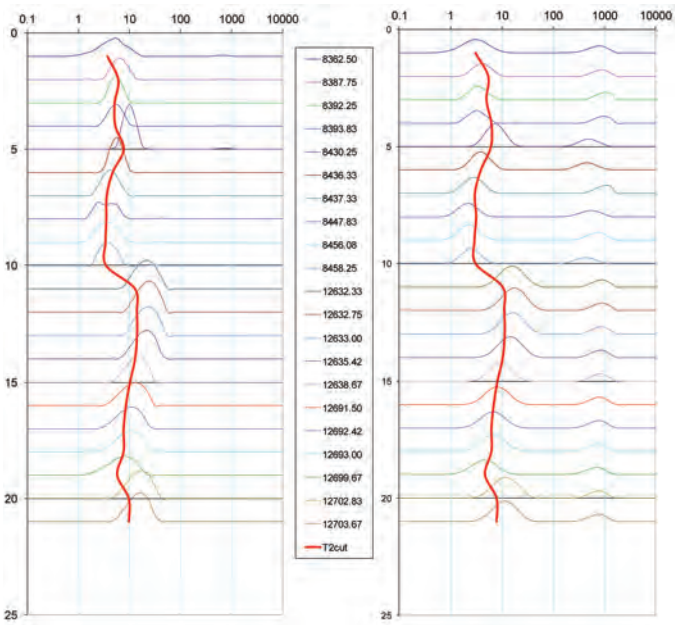

Fig. 11—NMR response as measured in the lab at S_w = 1 (left), and the simulated response as measured by NMR under actual reservoir conditions (right). The 8xxx samples are from Well A, the 12xxx from Well C. The vertical red line is the T_{2mean} of the samples (the offset is an illusion: the T_{2mean} is plotted vertically at the baseline of each sample, rather than at the top of the peak). Horizontal axis is T_2 (msec), and vertical are sample numbers with sample depth in the legend.

The effect on the correlation between $T_{2cutoff}$ and T_{2peak} is shown in Fig. 10. Under downhole conditions, there is still a good correlation, but it has shifted compared to the lab correlation of Fig. 10. Using the uncorrected correlation would result in significant overestimation of bound water.

The correlation found for the downhole conditions as encountered in Well A is:

T2_cutoff = A * T2_peak^B		Lab	in-situ
	A =	1.383	1.783
	B =	0.726	0.656

Permeability. Permeability prediction is one of the popular applications of NMR. This stems from the fact that NMR can distinguish between different pore sizes at any given porosity. Two correlations are widely used:

$$k_{Coates} = a(POR/10)^b(FFI/TBW)^c \quad (2)$$

$$k_{SDR} = a(POR/100)^b(T_{2mean})^c \quad (3)$$

where, POR is porosity in p.u.; T_{2mean} in msec; permeability, k, in md; FFI is the free-fluid index; TBW, total bound water.

While this is approach fairly successful for sandstones, the results are quite mixed for carbonates. The Coates relation uses the ratio of large pores and small pores. As pointed out above, the split between FFI and TBW is much more complicated in carbonates than in sandstones. Hence, using a fixed $T_{2cutoff}$ is likely to fail. The variable cutoff has some chance of success. The SDR relation simply uses the T_{2mean} of the T_2 distribution as a measure of the mean pore size. This may work better than the Coates relation in carbonates, but it suffers from the effects of the hydrocarbons on the NMR signal. See, for example, the change in T_{2mean} due to oil in Figs. 1 to 4. Using the modeling, we computed the optimum values of the parameters a, b and c in these two correlations. In Table 1, we first list the default parameters, including the fixed $T_{2cutoff}$ of 100 msec. Then, we optimized the parameters a, b and c for the samples as measured in the lab, i.e. at S_w = 1 (Fig. 12). Finally, we optimized the parameters for the modeled response at in-situ conditions (Fig. 13). In the latter case we used the variable $T_{2cutoff}$ derived above. Also note that the T_{2mean} in the SDR relation, when applied to the wireline NMR log, is that under the actual in-situ conditions; hence, the parameters should be based on similar data, i.e. simulated downhole conditions. Figure 14 shows the results that would be obtained when, erroneously, the lab calibration is applied to the samples at in-situ condition, i.e. to log data. Note that the false impression is given that the Coates permeability is not affected; this is because in this particular case, the NMR exponent C happens to be zero. In general, this is not so, and a similar discrepancy is seen. By applying the in-situ calibrated parameters, the predicted permeability on actual conditions (Fig. 13) is as good as that under laboratory conditions (Fig. 12).

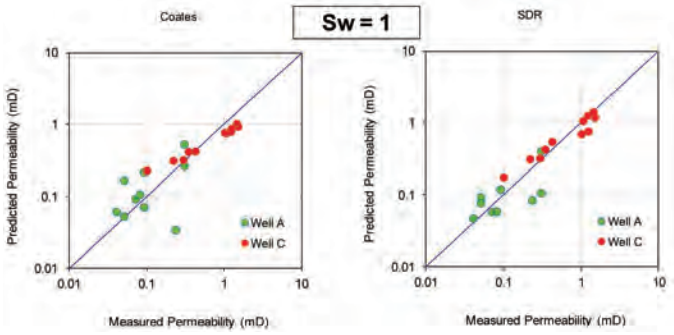

Fig. 12—Optimized permeability prediction for the samples at S_w = 1.

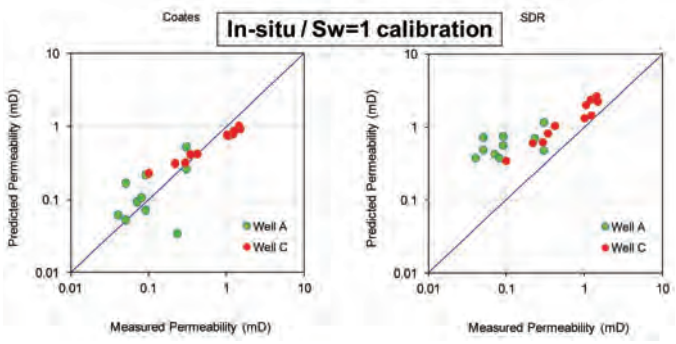

Fig. 13—Optimized permeability prediction for the samples at in-situ conditions as in well A.

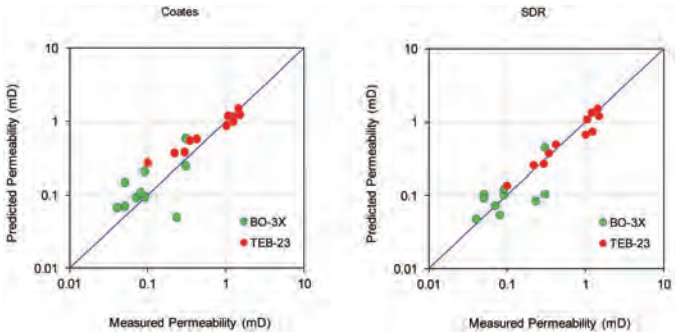

Fig. 14—Predicted permeability when using lab calibration on samples at in-situ condition.

It is interesting to note that the NMR exponent C has become zero for the $S_w = 1$ condition. This implies that, in contrast to the usual situation, there is no additional information to gain from NMR; there may still be a correlation between pore size and porosity, which explains why the porosity exponent is greater than the usual value of 4. For completeness' sake, also the generally used default parameter values are given.

Table 1—Permeability Prediction Parameters at In-Situ Conditions as in Well A

Permeability prediction						
	Coates			SDR		
	Default	@Sw=1	in-situ	Default	@Sw=1	in-situ
T2 cutoff =	100	95	variable	n/a	n/a	n/a
min_BVI =	1	1	1	n/a	n/a	n/a
pre-factor (A) =	1	0.0014	0.004	0.4	0.029	0.094
POR exponent (B) =	4	5.20	4.16	4	0.93	1.91
NMR exponent (C) =	2	0.00	0.60	2	1.56	1.00

An unavoidable implication of having to calibrate the permeability parameters against in-situ modeled data is that the calibration may change if the in-situ conditions differ from those in the model. The most important condition is S_{xo}, and thus the degree of flushing in the invaded zone by water filtrate. In the case of OBM, the bound water signal is clearly separated from that of the oil (filtrate and crude), which allows the application of the Coates permeability calibrated for $S_w = 1$ and a $T_{2\text{cutoff}}$ at an appropriate place between the water and oil peaks. The advantage of modeling over actual measurements is now obvious: any change in conditions can easily be made and the corresponding parameters are updated. This is not possible with laboratory experiments. Nevertheless, the latter are valuable to benchmark the model; once validated, it can be trusted to predict the correct response for the actual conditions encountered.

Derivation of Capillary Pressure Data from NMR. NMR distributions can be transformed into (pseudo) capillary-pressure curves using the method described in (Volokitin et al., 1999, Looyestijn et al., 1999). The transform requires a single parameter, kappa, κ, that combines the surface relaxivity and ratio of pore throat and body, as well as unit conversion (pressure and time). Because the ratio of pore throat and body is not constant over the entire range of pore sizes, κ is a function of either T_2 or P_c. Here we express the dependence as a function of T_2.

The calibration was made on the available core data. Out of these samples, there were 18 samples that have both NMR and mercury-injection capillary-pressure (MICP) data. After a first tentative calibration, it was found for some samples that their NMR and MICP data did not match very well. Since MICP was done on trim ends, it may well be that the trim ends differ from the main plug. These samples were given a reduced weight in the calibration.

The final conversion is shown in Fig. 15. It can be seen in several cases the NMR-derived capillary-pressure curve shows a good overlay of the MICP. Some samples show a poor fit; this could be because the trim ends differ from the main plug, or that there is another variable that is not picked up by the NMR response.

The corresponding variation of κ with P_c or T_2 is shown in Fig. 16. The calibrated parameter values are fairly normal for carbonates. A suitable, empirical, relation for κ as function of T_2 is given by

$$\kappa = \kappa_0 + \frac{\kappa_{\text{low}} - \kappa_0}{(1 + T_2/T_{2,flex})^{\alpha}} \qquad (4)$$

where κ_0 is the initial value (in psi.s), κ_{low} the κ value at low T_2, T_2 in sec, $T_{2,\text{flex}}$ the flexpoint in msec; the rate of change is determined by the exponent α. The parameter values found are shown at the bottom of Fig. 15. The parameter α controls the slope of the κ (T_2) function. Over the years, we found no reason to vary this parameter; therefore it is fixed in our software (its value is 9), and cannot be changed by the user.

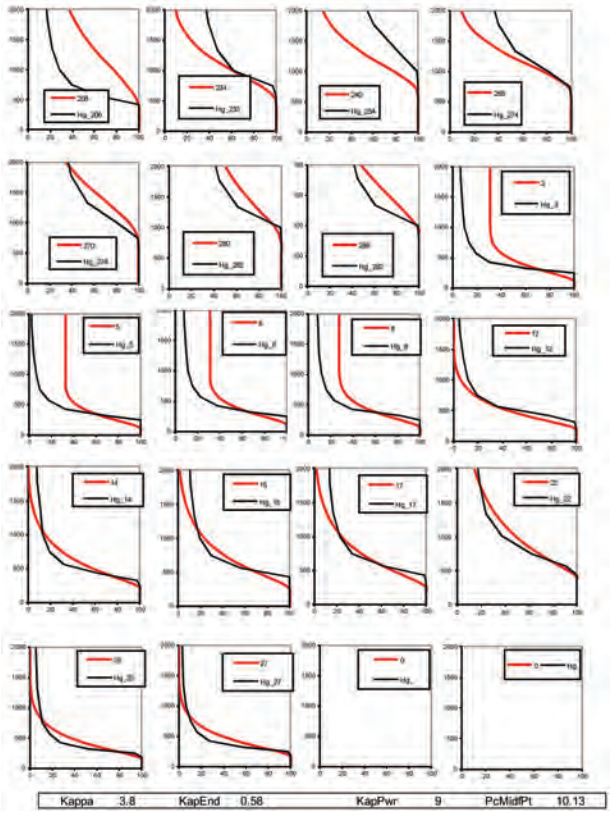

Fig. 15—Overlay of pseudo-capillary-pressure curves from NMR and actual MICP data. Horizontal axis is wetting phase saturation (%), and vertical is $P_c(Hg_{air})$ (psia).

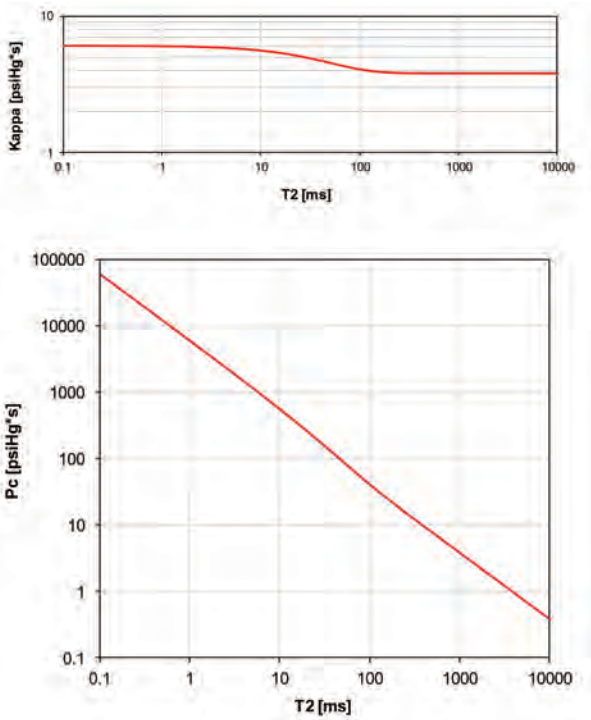

Fig. 16—Variation of κ with T_2 (top), and resulting relation between P_c and T_2 (bottom).

INTERPRETATION OF NMR LOG IN WELL A

The wireline NMR log in well A was obtained in 2008 with the Baker Hughes MREX tool. The data acquisition was done in PPLightOil mode. This mode employs a sequence of activations, covering a range of setting of parameters that affect the T_2 response, notably the interecho time, *TE*, the wait time (*TW*) and the number of echoes, *NE*. Because these activations are run subsequently at spatially separate volumes, also the operating frequency, depth of investigation, DOI, and the field gradient, *G*, vary. One complete sequence comprises 24 activations. An overview is given in Table 2, where the activations are grouped according to the activation parameter settings.

The PPLightOil acquisition allows for more advanced processing (Slijkerman et al., 1999), in particular to differentiate (light) oil from water. In the present case, this interpretation was not made, and only an undifferentiated T_2 distribution was available. As will be discussed further on, the separate contributions of oil and water can easily be recognized from this log.

Table 2—Parameter Values for the 24 Activations in the PPLightOil Sequence

	Suffix	NE	TE	TW	Grad	Freq	DOI
Long train	21	1000	0.4	11113	19.7	615.8	3.4
	23	1000	0.4	11111	16.9	556.6	3.7
	1	1000	0.4	9225	27.3	767.5	2.8
	5	1000	0.4	1010	27.3	767.5	2.8
	13	285	1.4	8272	32.5	862.2	2.5
	17	285	1.4	1038	32.5	862.2	2.5
	11	148	2.7	9194	23.3	690.0	3.1
	3	148	2.7	8291	38.5	965.0	2.2
	15	148	2.7	1033	23.3	690.0	3.1
	7	148	2.7	1011	38.5	965.0	2.2
Short (CBW or TP) trains	4	25	0.4	20	38.5	965.0	2.2
	8	25	0.4	20	38.5	965.0	2.2
	14	25	0.4	20	32.5	862.2	2.5
	18	25	0.4	20	32.5	862.2	2.5
	2	25	0.4	20	27.3	767.5	2.8
	6	25	0.4	20	27.3	767.5	2.8
	12	25	0.4	20	23.3	690.0	3.1
	16	25	0.4	20	23.3	690.0	3.1
	22	25	0.4	20	19.7	615.8	3.4
	24	25	0.4	20	16.9	556.6	3.7
BW trains	9	25	0.4	50	38.5	965.0	2.2
	19	25	0.4	50	32.5	862.2	2.5
	10	25	0.4	100	38.5	965.0	2.2
	20	25	0.4	100	32.5	862.2	2.5

A short section of the full NMR log is shown below to highlight a couple of features that will be addressed in the next sections.

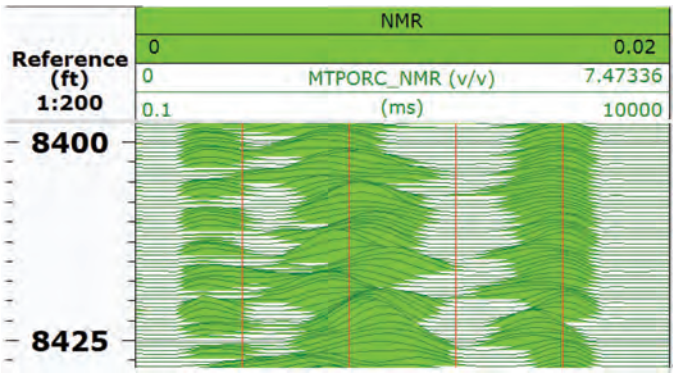

Fig. 17—Short section of the NMR log in well BO-3X showing the characteristic features in the oil zone: one peak below 1 msec, a second peak around 10 msec, and a third peak near 1 sec.

*Peak Below 1 msec.*The simulations presented above do not show a peak in the range below 1 msec, whereas this is prominently present in the NMR log. Since the core data were taken from the same well, it is hardly possible that all core samples are biased in the sense that they missed an important lithological feature. Relaxation times shorter than 1 msec are indicative of (sub-) microporosity and certain clay minerals. The amplitude of the peak is indicative of an abundance that cannot have been missed during sample selection.

Another, and indeed far more likely, explanation is that this peak is an artifact. In our experience, similar features are often seen, but usually not consistently over such a long interval. All NMR logging tools suffer from the same problem, which is sometimes attributed to ringing: a mechanically resonant vibration in the antenna after the activation pulse (Fukushima 1997). This must have died out before the echo appears. Apparently this is hard to control; a particular tool may function perfectly in one job, and have problems in the next. Another mechanism is spin dynamics in grossly inhomogeneous magnetic fields, which can be overcome by careful tuning of the pulse timing (Borneman et al., 2010).

Whatever the cause, the problem is manifested as a distortion on the first echo, much less on the next, and hardly at all on the subsequent echoes. Furthermore, it is more likely to occur for the shortest *TE* than for any longer value. Some vendors skip the first echo as a matter of routine in their standard processing. The presence of a ringing problem is not always easy to detect. In our processing we look for an abnormal out-of-phase signal, but if the ringing happens to be in phase with the true signal, it goes undetected.

To investigate this explanation, the echo data were examined. We made four subgroups of the data, combining the short trains, with *TE* = 0.4 msec, in one group (TP), and the long trains into three groups with *TE* = 0.4, 1.4 and 2.7 msec, respectively. Each group was then inverted into a single T_2 distribution. The inversion was done twice, first using all echoes, and second with omitting the first echo. The result is shown in Fig. 18.

The T_2 distributions with *TE* = 0.4 msec (Track 3 and 4) show a strong peak at very short T_2. This is not seen in the next two tracks, with *TE* = 1.4 and 2.7 msec, respectively. If this peak were genuine, it would have been seen in these tracks, be it with somewhat reduced amplitude. When the first echo is omitted in processing, this short T_{2peak} is largely gone. Therefore, it can be concluded that this very short T_{2peak} is an artifact cause by ringing of the first echo at the shortest *TE*.

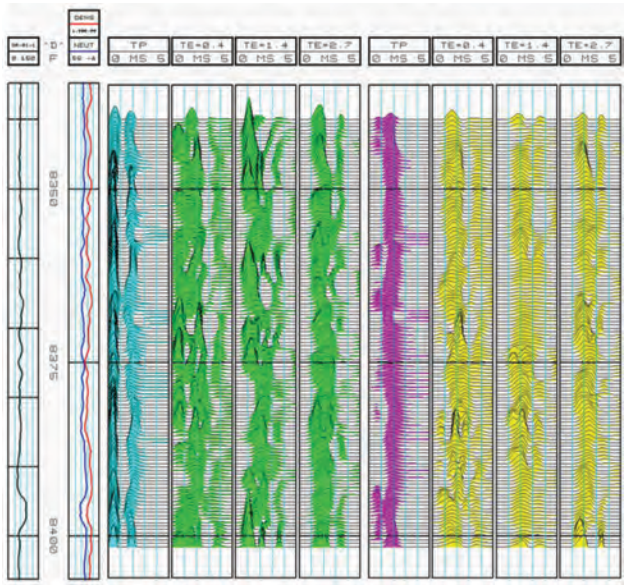

Fig. 18—Reprocessed NMR data. TP = short train (25 echoes, *TE* = 0.4 msec), the rest are long trains, with *TE* of 0.4, 14 or 2.7 msec. The first set of four distributions use all echoes, the second set has the first echo skipped.

To further explore this explanation, a simulation was made. Figure 19 shows that even a relatively small (positive) distortion of the first echo causes the appearance of an early peak in the distribution. This will always happen because of noise on the echoes. However, this noise is random, and each echo is in practice the average of many measurements. Nevertheless, occasional occurrences of such "noise" peaks are always seen, but not systematically over long intervals. Ringing artifacts, on the other hand, tend to be systematic. Figure 20 shows the effect of increasing *TE* on the detection sensitivity of a real peak at short T_2. When *TE* is larger than the T_2 of the peak, the apparent amplitude decreases. However, a genuine peak at ~ 0.5 msec will still be seen with *TE* = 1.4 msec, but not with *TE* = 2.7 msec.

Looking now at the T_2 distributions of the subgroups in

Fig. 18, the simulated features are present throughout. It can thus be concluded that the peak seen below 1 msec on the NMR log is an artifact, and should be ignored.

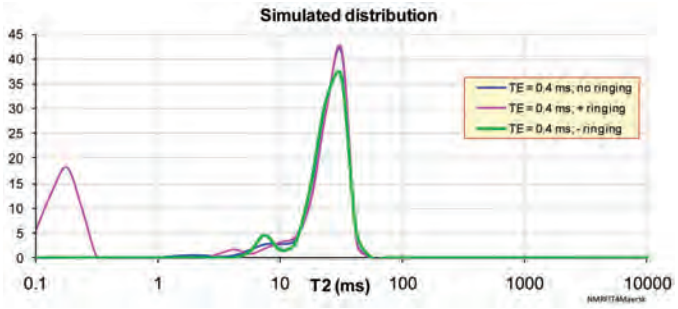

Fig. 19—Simulated response. The model has a single peak at around 30 msec. Increasing the first echo by 4% ("+ ringing") creates an artificial peak at 0.2 msec.

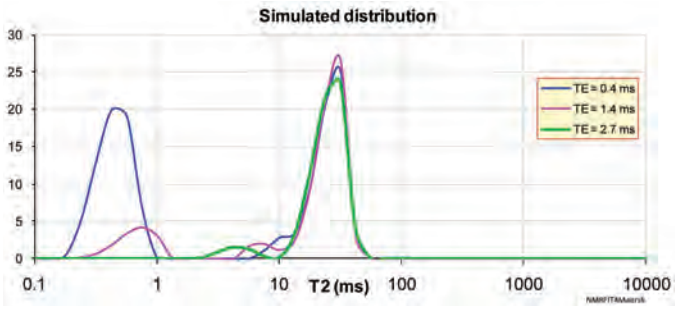

Fig. 20—This model has two peaks, as correctly shown with *TE* = 0.4 msec. Using longer *TE* values reduces the amplitude of the short peak.

The occurrence of this artifact is difficult to diagnose in the field. In reprocessing it could have been identified, but not remedied. All one can do is ignore the first echoes, which also removes any genuine information at very short T_2. In the present case, however, this can safely be done as there is sufficient evidence that there is no signal at such short T_2.

Modeling Desaturation By Humidity-Controlled Drying. The selection of the core samples were measured at S_w = 1 and then after humidity controlled drying. At the latter conditions, all samples show a peak at around 0.2 to 0.4 msec, which is remarkably similar to what is observed in the wireline NMR log in the same well. For a while it was thought to point to an explanation of this feature.

However, this peak cannot explain the peak seen on the wireline NMR log. First, this saturation is fairly low, between 0.6 and 1.2 % bulk volume (BV). Second, it only occurs when the water saturation is as low as around 0.3 %, corresponding to the mentioned 0.6 to 1.2 % BV. We used our modeling to demonstrate the effect on an arbitrary sample in Fig. 21. All other samples show the same behavior. In these plots, the water saturation is gradually decreased to 0.68, 0.30 and finally to 0.05. The decreasing saturation results in a decreased amplitude, but also in a shift to shorter T_2. As explained earlier, this is because the water volume goes down, while the surface area remains the same. Note that this short T_{2peak} is more than a factor of ten away from the fully saturated peak, yet, precisely at the actual low saturation, we find a full match with the actual measurement. The perfect correspondence between the modeled result and the actual measurement at desaturated condition is really remarkable, bearing in mind that the modeling has only been verified for water saturations down to normal irreducible values.

In the reservoir, the rock never gets to such low water saturations; the lowest one might expect is closer to the simulation given in Fig. 21, which shows no signal at very short T_2.

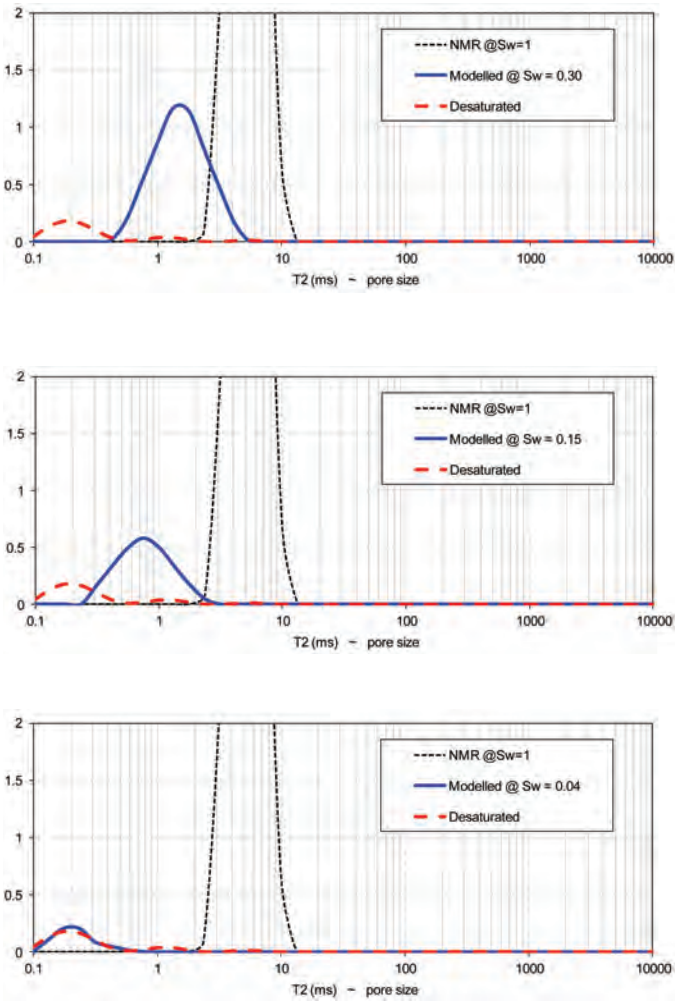

Fig. 21—Sample 240. Modeled NMR response of the water fraction at progressive desaturation levels. At S_w = 0.05 the same modeled response is found as is actually measured at that saturation.

COMPARISON OF MODELING AND ACTUAL NMR LOG IN WELL A

Figure 22 shows a short section of the NMR log in well A on a standard T_2 scale, plotting logarithmically from 0.1 to 10,000 msec; the two tracks show the same log with NMR core data at $S_w = 1$, and at simulated in-situ conditions, respectively. The core data are plotted at their corresponding (shifted) loggers depths. Obviously, the core data at $S_w = 1$, as measured in the lab and shown here in light blue, fail to show the oil peak at long T_2. The modeled result, shown in yellow in the last track, does show the oil peak. In the modeling, we anticipated the result for wettability and oil saturation that is discussed later. The correspondence between modeled result and the actual log is generally good. The peaks in the modeled responses are a bit sharper than what is seen in the log; this is due to the noise in the log data that results in a stronger regularization in the inversion that computes the T_2 distribution from the measured echoes.

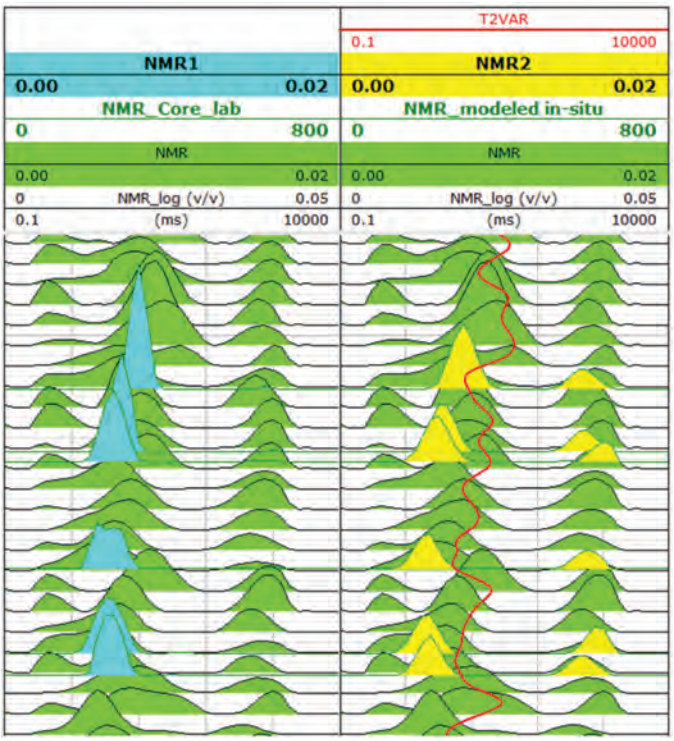

Fig. 22—NMR log in Well A with NMR core data at $S_w = 1$, and at simulated in-situ conditions.

Note that the core data does not feature the peak at short T_2, because this is an artifact in the log as discussed earlier in this paper. A full display of the results in Well A is presented in Fig. 23.

Porosity and permeability. NMR porosity (*POR_NMR*) does not require any post-processing other than a correction for the hydrogen index (*HI*). The liquids in well A all have *HI* close to unity, and no correction was applied. Track 7 shows that *POR_NMR* compares well with *PHIT_D*. Core porosity, *CPOR*, is not corrected for in-situ stress; it has some scatter due to small scale variability, but generally the agreement is satisfactory.

In the first part of this paper several permeability estimators were reviewed on the basis of the available core data, and calibrations were made for lab and in-situ conditions. The estimators were applied to the NMR log in Well A. The resulting permeability curves are displayed in Tracks 8 and 9 and compared against core data. Since the calibration was done against unstressed permeability, the result will be not stress-corrected. Using the default carbonate parameters grossly overestimates permeability; these results are not shown.

Using the calibration against the core data at $S_w = 1$ results in the curves in Track 8 with suffix lab. *PERM_SDR* is far too large; this is because the presence of oil significantly increases T_{2mean}. Interestingly enough, *PERM_COATES* is much closer to the core data. Inspection of the parameters in Table 1, however, reveals that the NMR exponent, C, is zero, which implies that the shape of the T_2 distribution is fully ignored in this particular case. In fact, what remains is a k-φ correlation, which is not affected by the presence of oil.

Track 9 shows the result of using parameters calibrated against the simulations for in-situ conditions; these curves have suffix var. For the Coates permeability, first the T_2 of the main (water) peak, T_{2peak}, was computed. Then, the variable $T_{2cutoff}$ was computed as defined earlier. This curve, T_2VAR, is shown as overlay on the T_2 distribution in Track 6. It can be seen that it tends to run at a little higher T_2 than the peak, but less higher where the peak is at a higher T_2. This is in line with the expectation that the finer rock has more bound water than the (relatively) coarser rock. Using this variable cutoff, the bound-water to free-fluid ratio was computed, and finally the Coates permeability with the appropriate parameters. The SDR permeability follows from the T_{2mean} and the in-situ parameters. The two estimations agree with each other very closely, and also compare well with the core data.

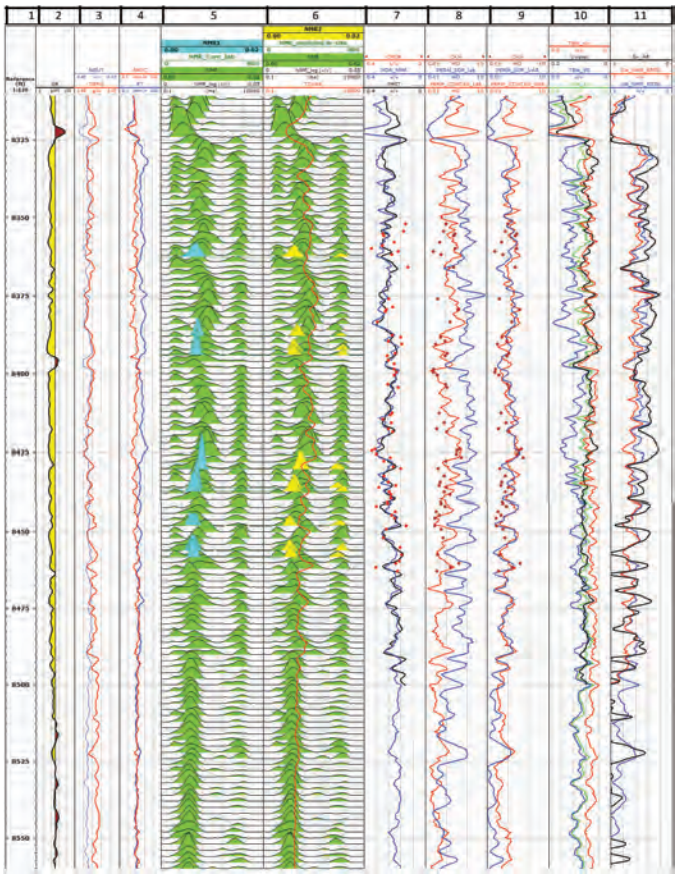

Fig. 23—NMR interpretation in Well A. The variable $T_{2cutoff}$ (Track 6) is based on a calibrated correlation with the peak of the water peak and gives a better S_w than a fixed cutoff (Track 10). The NMR capillary-pressure saturation (Track 11) indicates a deeper FWL than reached in this interval.

Saturation Calculations Using $T_{2cutoff}$. The NMR log can be used in several ways to compute/predict saturations. One saturation is the actual saturation that the NMR log sees, i.e. in the invaded zone at a few inches deep. This shallow S_{xo} will be discussed in the context of the wettability determination further on.

A more interesting saturation is the irreducible saturation. NMR logging derives part of its value from its ability to provide this information independent of resistivity logs. The only parameter needed is the $T_{2cutoff}$. However, it should be realized that this cutoff is normally calibrated against core data where S_{wirr} was obtained by a procedure (centrifuge, porous plate) that establishes a certain capillary pressure. In most rocks, in particular sandstones, the saturation curve has become virtually constant at this pressure, hence the name irreducible. In tighter rock, such as chalks, this may not be the case. In any case, such derived saturations refer to a single capillary pressure, and are expected to deviate from the actual saturation in the transition zone. One way to look at it is that it gives the maximum hydrocarbon saturation possible under fluid pressures up to the experimental condition; hence the name free-fluid index.

In the present case, however, there are no core data for S_{wirr} at all. Instead, the *SWT* curve, derived from resistivity, was used to estimate S_{wirr}, bearing in mind possible errors in depth match and the large difference in sample size between core and logs. The consequence of following this approach is that the NMR result cannot be used any longer as an independent verification of *SWT*.

Whereas in sandstones a single cutoff can be used, this does not work in the present situation, as discussed earlier in this paper. Instead, a variable cutoff is required, and it was found that this can be derived from a correlation with the T_2 of the peak in the T_2 distribution; the correlation was calibrated using the in-situ modeling.

The resulting saturations are given in Track 10 of Fig 23 in the form of water volumes (fraction of bulk) and compared against the result from resistivity, V_{water} = *PHIT* * *SWT*. The values obtained with a 95 msec cutoff, *TBW_95*, are far too high. An attempt was made to find a better match by lowering the cutoff; a cutoff of 15 msec gives a reasonable visual agreement between *TBW_15* and V_{water}, but clearly not everywhere. In contrast to a fixed cutoff, the result obtained with the variable cutoff, *TBW_var*, shows a good agreement with V_{water} over most of the interval. This demonstrates that the cutoff is indeed variable and it can also be predicted from the NMR log itself at every depth.

Saturation Calculations Using NMR capillary-pressure curves. The calibration given in Fig. 15 was used to convert the NMR log into capillary-pressure curves, and to derive saturations for three arbitrary values of the FWL. The result is shown in Track 11 for water saturation. It would seem that the real FWL may be somewhat deeper the bottom of this interval shown. Note that the conversion to capillary-pressure curves is purely based on core data, and therefore the saturations derived from them are independent of those derived from resistivity.

Comparison of NMR Saturation Prediction. As mentioned above, saturation prediction from NMR is generally successful in sandstones, but less so in carbonates. The saturations obtained in the previous two sections, therefore, were derived from more advanced techniques, namely variable cutoff and capillary-pressure curves. Inspection the results in Track 11, shows that a reasonable match is obtained, which can be taken as strong supporting evidence for the correct level of the saturation. However, significant deviations do occur that are not readily attributable to obvious errors in any of the logs.

WETTABILITY DETERMINATION

The principle of wettability determination by NMR relies on the fact that the wetting phase has an accelerated relaxation via its contact with the rock surface (Looyestijn 2005, 2008). The 100% end-members are the NMR responses of bulk water and bulk oil, and rock at $S_w = 1$ and at $S_o = 1$. If these are known, the actual NMR response can be interpolated between these for a certain value of S_w and the fraction of the rock surface that is water-wet or oil-wet, respectively. The NMR wettability index is then defined as:

$$I_w = \frac{Surface\ wetted\ by\ water - Surface\ wetted\ by\ oil}{Total\ Surface} \quad (5)$$

To conform to existing indices, I_w has been scaled from +1 for fully water-wet, through 0 for neutral, to -1 for fully oil-wet. It is emphasized that the definition of I_w has not more than only some resemblance with the traditional Amott and USBM indices. Since it is based on entirely different physics, there is no fundamental equality implied. The appropriateness of I_w as a predictor, or even replacement, of the traditional indices has been validated, both for core and log data).

It has been shown (Looyestijn 2005) that the absolute values of the surface relaxivity of water and oil are not required, but only their ratio $R = \rho_{Oil}/\rho_W$. This ratio can easily be determined on core samples. If these measurements are not available, or impossible, a default value of R = 0.3 is appropriate for limestone, and hence, possibly, for chalk.

A complication with log data is that one of the end-members, the response at $S_w = 1$, is not readily known. In the present case, the solution was found in taking the core data as reference. The modeling software finds for every log depth the core sample that is most representative with respect to its porosity; subsequently, the T_2 distribution is allowed to shift along the T_2 axis (i.e. changing its T_{2mean}). The in-situ response is now computed in the same way as described in the early part of this paper for a given value of S_w and wettability. These three parameters, T_{2mean}, S_w and wettability, are now adjusted to find a best fit of the predicted T_2 distribution with what was actually measured. The result of the modeling is thus not only a wettability index, but also an S_w (in fact, S_{xo} at a DOI of a few inches), and a hydrocarbon-corrected T_2 distribution. The latter is also used to predict permeability using the SDR equation with the parameters defined earlier.

It is important to note that the input curves for S_w and permeability are only used to provide a starting value for the fitting routine. The input T_2 distribution drives the solution that is characterized by the output distributions, oil saturation and wettability.

Figure 24 presents a short expanded-scale section of the full wettability analysis for Well A presented in Fig. 25. The first track with T_2 distributions shows the actual log (TPOR) overlain by the modeled version (FITMOD). As can be seen, the correspondence is generally good. In line with the conclusion earlier in this paper, the modeled result does not show a peak at short T_2 near 0.5 msec. At the top of the display in Fig. 25, the response of the bulk oil is shown as it would have been measured under the prevailing conditions and acquisition parameters. It can be seen that its location in T_2 is only a little higher than the right-hand peak that features throughout the NMR log. This is a qualitative indication that the rock is close to water-wet.

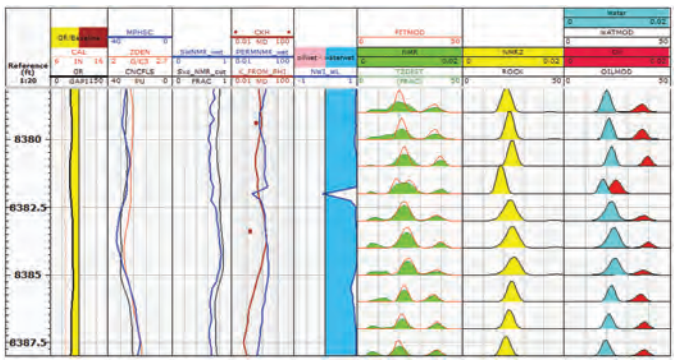

Fig. 24—Short section of the wettability interpretation result in Well A. The wettability index, *NWI*, is close to +1 indicating water-wet. The result of the modeling, FITMOD, matches the actual log, *T2DIST*, quite well with a few exceptions where the fit is erroneous. ROCK is the NMR distribution as it would be at $S_w = 1$.

Occasionally, the fitting procedure failed completely, resulting in a poor fit; these can easily be recognized and should be ignored. This happens, for example, at 8,382 ft, with *NWI* = ~0; however, the fit is poor and thus not reliable. The next track shows the hydrocarbon-corrected T_2 distribution, ROCK. The shape of the distributions was derived from the core data set, but their location on the T_2 axis may have been adjusted. The last two tracks show the water and oil T_2 distributions, respectively. Added together, they form the modeled response that overlays the actual log.

The actual, quantitative, wettability index is given in the track headed *NWI*. The index is very close to +1, corresponding to a water-wet state. This, fairly extreme, condition implies that the interpretation is rather insensitive to errors in the parameters used. Reducing $R = \rho_{Oil}/\rho_W$ from 0.3 to a rather low value of 0.1 results in a *NWI* of around +0.9, i.e. still very water-wet. Similarly, significant variation in the oil viscosity can be allowed without changing the interpreted wetting condition.

Finally, the S_w values found (S_{xo}—*NMR*) correspond closely to the starting values (S_{xo}); however, this was to be

expected as this S_{xo} curve was derived by integrating the NMR response above 100 msec, i.e. anticipating that the long peak is oil and the rest water. The predicted permeability, *PERM_NMR*, is also close to the input permeability that was derived from the k-ϕ correlation. The selected core samples have a good k-ϕ correlation, which is preserved in the modeling. Obviously, the wettability interpretation has no value in intervals that have no oil. This happens above the reservoir (~8,325 ft), but also at a few short intervals within the reservoir section and in the water leg.

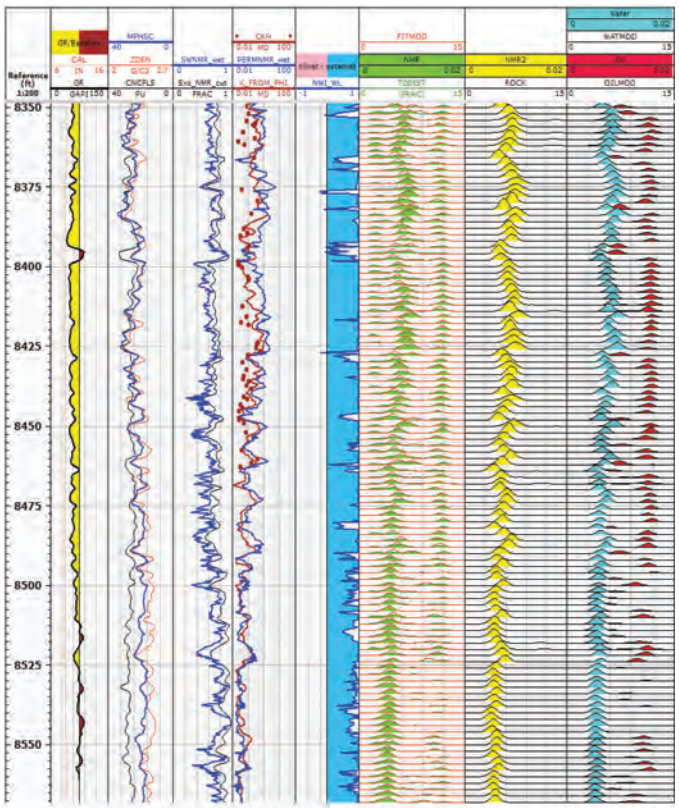

Fig. 25—Wettability interpretation result in Well A. The index *NWI* is close to +1, indicating water-wet. The result of the modeling, FITMOD, matches the actual log, *T2DIST*, quite well with a few exceptions where the fit is erroneous. ROCK is the NMR distribution as it would be without oil.

LWD-NMR DATA IN WELL B

Well B was logged-while-drilling in OBM in 2011 using the Baker Hughes MagTrak tool. This well is easier to interpret because the oil filtrate does not change the water saturation; the bound-water signal is clearly separated from that of the crude oil and OBM filtrate. The oil signal, on the other hand, is now more complicated because it is an unknown mix of native crude and oil filtrate.

After completion of the previous chapters, new data was acquired in well B. This well was drilled with OBM, and the NMR data were acquired while drilling the horizontal section. As mentioned above, invasion of OBM filtrate will not change the water saturation or the NMR signal of the (bound) water. The forward modeling predicted a clear separation between the water and the oil signal, even if the oil would be a mix of filtrate and initial crude oil. This is indeed what is observed over the entire length of the logged interval (10,800 to 20,200 ft). Fig. 24 shows a short interval to illustrate the interpretation principle; the same is valid for the rest of logged interval.

The logged NMR distribution is overlain with a few modeled responses. These were based on core samples that have similar high porosities; the saturation, however, were taken from the interpreted NMR log as discussed below. It was assumed that no filtrate is present, and that the wettability is similar as in Well A (i.e. water-wet). It can be seen that the match between actual log and modeled response is very good. More recent information indicates that the base oil of the mud has an in-situ viscosity of approximately 0.75 cp; this corresponds to a T_2 of nearly 2 sec. This is very close to the estimated T_2 of the crude oil. Hence, the "oil" T_{2peak} can be anything from pure crude to pure filtrate, or any mix in between. This would not affect the NMR interpretation, and in particular not NMR porosity because both fluids have a hydrogen index of close to unity. The amount of filtrate may affect the density log because the filtrate is denser than the crude.

The calculation of water and oil saturation, S_{wi} and S_{oil}, respectively, is now straightforward. We applied a variable $T_{2cutoff}$, defined as the T_2 value in the centre of the trough between the water and the oil peak. The integrated signal at either side gives the water and oil volumes, and corresponding saturations after division by their sum. It appears that the trough between the peaks is rather wide, and virtually the same results are obtained by a using a fixed $T_{2cutoff}$ at 25 msec.

In Well A there is overlap between water and oil, and that is exactly why a variable $T_{2cutoff}$ is required when WBM is used. In Well B there is clear separation and that is very common with OBM, unless the crude is rather heavy. That is the usual case where cutoffs normally fail. The modeling presented here might help; this requires assumptions on the rock as explained in (Looyestijn, 2008).

A assessment of the presence of mobile water cannot be made from these NMR log data alone. As the modeling showed, the water signal at any S_w level is a single peak between approximately 1 and 10 msec. Invasion of OBM filtrate will have moved any moveable water; in that case, S_w from NMR is lower than that from resistivity. If they are

equal, the presence of mobile water is unlikely.

Permeability is now computed using the Coates formula with the parameters defined in the lab (apart from the $T_{2cutoff}$; that is as discussed above). Note that the in-situ calibration is not required because the water signal remains unaltered by filtrate invasion. Any OBM filtrate invasion may move the T_2 of the combined oil peak, but not its volume. In this particular instance, the *FFI/PORT* exponent happens to be zero, which makes the permeability a function of porosity only. This is rather exceptional, and in other fields there may be a non-zero NMR exponent.

The interval shown at the top of Fig. 26 (13,050 to 13,115 ft) has a higher gamma-ray reading and a shale separation on the neutron-density logs. NMR porosity, MPHS, is significantly less than neutron porosity. This is all consistent with a shale interval. However, shales normally have a T_2 response around a few msec only, and not a second peak around 100 msec. This could be OBM filtrate, but the volume is much greater than what would be expected for an impermeable shale, even for a low-permeability silt. Note that the computed permeability may not be valid over these intervals.

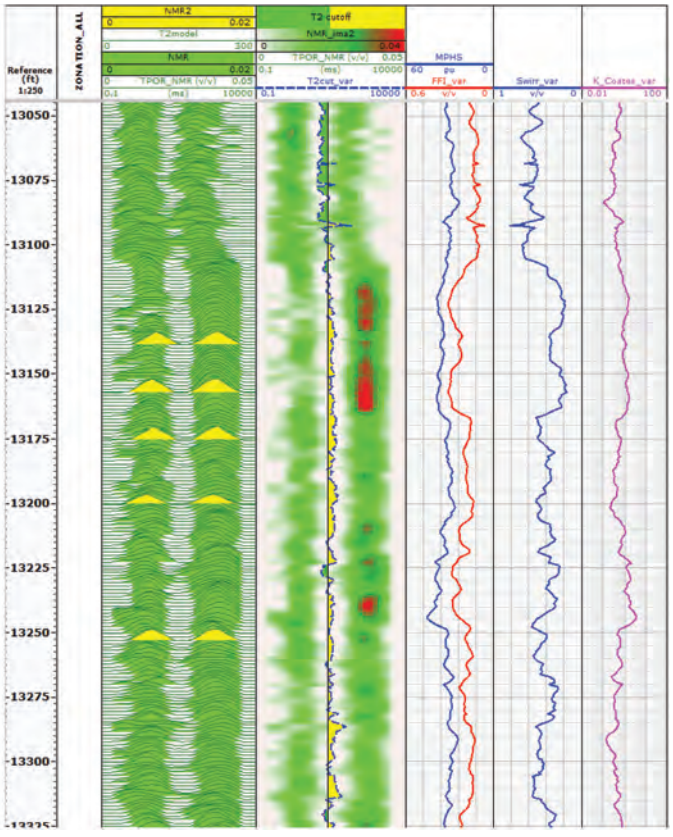

Fig. 26—Short interval of the LWD NMR log taken in Well B and interpreted results.

CONCLUSIONS AND RECOMMENDATIONS

This study on the interpretation of the NMR log taken in Wells A and B has lead to the following findings:

- NMR response at full in-situ conditions, including effects due to the presence of oil and to specific hardware features, has been obtained by forward modeling. A good match between modeled results and the NMR log has been achieved in both WBM and OBM wells.
- The peak seen at short T_2 of approximately 0.5 msec, is not reproduced by the forward modeling results—it is most likely an artifact due to ringing of the first echo. This is substantiated by in-house processing of the data, revealing that this peak is only seen with the shortest interecho time, and not with a longer one. Additional evidence is that none of the core samples shows this short peak.
- The peak seen at long T_2 of just below 1 sec is attributed to oil at a remaining saturation of approximately 30%.
- Wettability was assessed from the shift of the oil relaxation time away from its predicted bulk value under reservoir conditions. The reservoir appears to be strongly water-wet in both wells.
- Above modeling was used to calibrate a variable $T_{2cutoff}$ for the prediction of bound water from the NMR log. The result compares generally well with the resistivity derived saturation.
- Pseudo-capillary-pressure curves were computed from the NMR log, using calibration against available core data. This method allows prediction of saturation as function of height above an assumed FWL, rather than at a constant pressure, as is done using a $T_{2cutoff}$.
- The parameters for the NMR permeability predictors were calibrated for reservoir conditions. Excellent agreement with core data was found.

NOMENCLATURE

BV	= bulk volume
CPOR	= core porosity
FFI	= free-fluid index, fraction bulk volume
HI	= hydrogen index
I_w	= wettability index
k	= permeability, md
κ	= conversion factor, psi.s
κ_{low}	= value for κ at short T_2
κ_0	= value for κ at long T_2
MPHS	= NMR porosity
NE	= number of echoes
NWI	= wettability index

OBM = oil-based mud
P_c = capillary pressure, psi
PERM_NMR = NMR permeability, md
PERM_COATES = NMR permeability according to Coates, md
PERM_SDR = NMR permeability according to SDR, md
PHIT = total porosity, fraction bulk volume
PHIT-D = total porosity from density, fraction bulk volume
POR = porosity, fraction bulk volume
POR_NMR = NMR porosity, fraction bulk volume
PORT = NMR porosity, fraction bulk volume
R = pore radius, m
ROCK = T_2 distribution @ Sw = 1
S_{xo}*_NMR* = water saturation derived from NMR
S_w = water saturation
S_{wirr} = irreducible water saturation
S_{xo} = invaded-zone water saturation
SWT = virgin formation water saturation
T_2 = relaxation time, sec
$T_{2,D}$ = diffusion decay time, sec
$T_{2cutoff}$ = cutoff in T_2, msec
T_{2mean} = logarithmic mean of T_2 distribution, msec
T_{2peak} = peak (mode) of T_2 distribution, msec
T2DIST = T_2 distribution
T_2*VAR* = variable $T_{2cutoff}$
TBW = *total bound water, fraction bulk volume*
TBW_15 = TBW using $T_{2cutoff}$ = 15 msec
TBW_95 = TBW using $T_{2cutoff}$ = 95 msec
TBW_var = TBW using $T_{2cutoff}$ = variable
TE = interecho time, sec
V_{water} = water volume, fraction bulk volume
WBM = water-based mud
α = exponent in κ formula
ϕ = porosity, fraction bulk volume
ρ_{Oil} = density oil, g/cm^3
ρ_W = density water, g/cm^3

REFERENCES

Borneman, T.W., Hürlimann, M.D., and Cory D.G.J., 2010, Application of Optimal Control to CPMG Refocusing Pulse Design, *Journal of Magnetic Resonance*, **207**(2), 220-33.

Fukushima, E., and Roeder, S.B.W., 1979, Spurious Ringing in Pulse NMR, *Journal of Magnetic Resonance*, **33**(1), 199-203.

Lo, S.W., Hirasaki, G.J., House, W.V., and Kobayashi R., 2000, Correlations of NMR Relaxation Time with Viscosity, Diffusivity, and Gas/Oil Ratio of Methane/Hydrocarbon Mixtures, Paper SPE 63217, presented at the 2000 SPE Annual Technical Conference and Exhibition, Dallas, Texas, October 1-4.

Looyestijn, W.J., 2008, Wettability Index Determination from NMR Logs, *Petrophysics*, **49**(2), 130-145.

Looyestijn, W.J., and Hofman, J.P., 2006, Quantitative Wettability Index Determination by Nuclear Magnetic Resonance, Paper SPE 93624, *SPE Reservoir Engineering and Evaluation*, **9**(2), 146–153

Looyestijn, W.J, Volokitin, Y., Slijkerman, W.F.J., and Hofman, J., 2001, A Practical Approach to Obtain Primary Drainage Capillary Pressure Curves from NNR Core and Log Data, Paper SCA 9924, *Petrophysics*, **42**(4), 334-343..

Slijkerman, W.F.J., Looyestijn, W.J., Hofstra, P., and Hofman, J.P., 2000, Processing of Multi-Acquisition NMR Data, Paper SPE 68408, *SPE Reservoir Evaluation and Engineering*, **3**(6), 492-497.

Volokitin, Y., Looyestijn, W.J, Slijkerman, W.F.J., and Hofman, J., 1999, Constructing Capillary Pressure Curves from NMR Log Data in the Presence of Hydrocarbons, Paper KKK, *Transactions* SPWLA 40th Annual Logging Symposium, Oslo, Norway, May 30 – June 3.

ABOUT THE AUTHORS

Wim Looyestijn obtained a PhD from the University of Leiden and has worked with Shell in petrophysical research for a third of a century. While he published on a variety of subjects, his main interest is in developing NMR applications such as fluid differentiation by diffusion and wettability. He was Editor of *Petrophysics* in 2007/2009, and has been president of the Dutch Petrophysical Society since 2000.

Stefan Steiner obtained a MSc from the University of Giessen and works in Maersk Oil. For the last five years he has been in charge of the petrophysical modeling in the Lower Cretaceous reservoirs in Denmark. Prior to joining Maersk Oil in 2007, Stefan had a 10- year career with Shell International with postings in The Netherlands and Nigeria. He is a member of SPWLA, AAPG and SPE.